

THE IMPACT OF VITAMIN D DEFICIENCY AND SEX HORMONE IMBALANCE ON THE CEREBROVASCULAR SYSTEM

PhD thesis

Dorina Nagy, PharmD

Semmelweis University Doctoral School
Theoretical and Translational Medicine Division



Supervisor: Éva Pál, PharmD, PhD

Official reviewers: Levente Sára, MD, PhD
 Ákos Menyhárt, PhD

Head of the Complex Examination Committee:
 György Reusz, MD, DSc

Members of the Complex Examination Committee:
 Zoltán Prohászka, MD, DSc
 Mihály Kovács, DSc

Budapest
2023

1. Introduction

Despite the growing concerns, vitamin D deficiency (VDD) still affects 24-40 % of the population. Vitamin D regulates several physiological functions related to cardiovascular health, mainly by regulating gene expression. For instance, it modulates endothelial function, immune and inflammatory responses, oxidative stress, cell proliferation and differentiation, and extracellular matrix homeostasis. Consequently, VDD is associated with endothelial dysfunction, accelerated atherosclerosis, impaired vascular reactivity, and adverse arterial remodeling. Thus, VDD has been linked to the increased risk of cerebrovascular disorders, including ischemic stroke, which frequently develops due to carotid artery stenosis. When a large artery is blocked, the blood is redistributed *via* the arteries of the circle of Willis. In addition, leptomeningeal collaterals provide an alternative route to deliver blood to unsupplied areas; thus, their number and condition significantly affect the outcomes of an occlusion. Epidemiological studies suggest gender differences in the prevalence of cerebrovascular disorders: men have been reported to have higher incidence and mortality rates than women. However, postmenopausal and hyperandrogenic women (e.g. women with polycystic ovary syndrome) appear to have higher risks of cerebrovascular disorders compared to healthy women, and their health condition is often accompanied by VDD, which might further aggravate the cardiovascular consequences of altered hormone status. Sex steroids, particularly estrogen and androgens, exert significant and probably opposing effects on the cerebrovascular system and, therefore, on the regulation of cerebral blood flow. For instance, estrogen promotes endothelium-dependent vasodilatation and protects against vascular inflammation, whereas long-term exposure to testosterone can lead to vasoconstriction, vascular inflammation, and oxidative stress. Although both optimal vitamin D and sex hormone status have been associated with cerebrovascular health, it is still unclear how sex

hormones and their imbalance (i.e., estrogen deficiency and androgen excess) influence the cerebrovascular consequences of VDD.

2. Objectives

We have recently demonstrated the severe functional consequences of disrupted vitamin D signaling in the adaptation of cerebral microcirculation to unilateral carotid artery occlusion (CAO) in male mice. Furthermore, we reported the significance of well-preserved pial collateral circulation in efficient cerebrocortical blood flow (CoBF) compensation following CAO. However, extracranial vessels, for instance, the contralateral carotid artery, may also play an important role in the adaptation to unilateral CAO. Therefore, our first goal was to examine the impact of vitamin D receptor (VDR) inactivity on the compensatory increase in blood flow in the contralateral carotid artery after unilateral CAO in male mice.

Considering the lower vulnerability of women to cerebrovascular disorders, we hypothesized that premenopausal healthy females may be more protected from the harmful effects of VDD compared to males, implying a protective role of estrogen in the cerebrovascular consequences of VDD. Therefore, we aimed to investigate the impact of VDR inactivity on the

- efficiency of the cerebrovascular adaptation to CAO,
- morphology of leptomeningeal collaterals and
- extracranial collateral circulation in healthy females.

Additionally, we hypothesized that estrogen deficiency or androgen excess in females might aggravate the cerebrovascular consequences of VDD. Therefore, our next goal was to investigate the efficiency of the cerebrovascular adaptation to CAO in ovariectomized and hyperandrogenic VDR-mutant female mice.

3. Methods

3.1. Experimental design

The experiments were performed in adult male and female mice carrying functionally inactive vitamin D receptors (VDR Δ/Δ) and their wild-type (WT) littermates on a C57BL/6 genetic background, bred by intercrossing heterozygous animals. The animals were housed in a specific pathogen-free facility at constant temperature (19-22 °C) with a 12/12 light/dark cycle, and they had ad-libitum access to chow and water. To ensure normal calcium homeostasis, all animals were fed with a specific chow (so-called rescue diet) enriched with calcium (2%), phosphorus (1.25%), and lactose (20%). The mice were involved in the experiments at the age of 90-120 days. Table 1 summarizes our experimental design. All procedures were approved by the National Scientific Ethical Committee on Animal Experimentation (PEI/001/2706-13/2014, approval date: 17 December 2014; PE/EA/00487-6/2021, approval date: 9 November 2021) and were conducted according to the guidelines of Hungarian Law of Animal Protection.

Table 1. Experimental groups and the measurements conducted on them.

Group	WT	VDR Δ/Δ	OVX-WT	OVX-VDR Δ/Δ	TT-WT	TT-VDR Δ/Δ	WT δ	VDR Δ/Δ δ
Sex	♀	♀	♀	♀	♀	♀	♂	♂
Disrupted vitamin D signaling		✓		✓		✓		✓
Ovariectomy			✓	✓				
Testosterone treatment					✓	✓		
Vaginal cytology	✓	✓	✓	✓	✓	✓		
Cerebrocortical blood flow measurement	✓	✓	✓	✓	✓	✓		
Carotid artery blood flow measurement	✓	✓					✓	✓

Morphological analysis	✓	✓						
------------------------	---	---	--	--	--	--	--	--

3.2. Ovariectomy and testosterone treatment

At three months of age, bilateral ovariectomy (OVX) was performed in 10 VDR^{ΔΔ} and 10 WT female mice under isoflurane (2%) anesthesia (OVX-VDR^{ΔΔ} and OVX-WT groups), whereas 10 VDR^{ΔΔ} and 10 WT mice received daily transdermal testosterone treatment (0.033 mg/g b.w., Androgel 1%) for five weeks (TT-VDR^{ΔΔ} and TT-WT groups) to induce androgen excess. The effectiveness of the testosterone treatment was examined by measuring testosterone concentration using ultra-high performance liquid chromatography-tandem mass spectrometry in serum samples separated from arterial blood collected after the *in vivo* cerebrocortical blood flow measurements. Body weight was measured before OVX/at the beginning of testosterone treatment and five weeks later to determine weight gain.

3.3. Vaginal cytology

Vaginal cytology was examined in intact, ovariectomized, and testosterone-treated VDR^{ΔΔ} and WT female mice for at least five consecutive days before performing the *in vivo* cerebrocortical blood flow measurements. In the early mornings, vaginal smears were collected from awake animals by flushing the vaginal canal with 0.1 mL saline solution using syringes with blunt needles. The stage of the estrus cycle was determined by evaluating the proportion of leucocytes, cornified epithelial cells, and nucleated epithelial cells in unstained samples under light microscopy. In the ovariectomized groups, the successful removal of the ovaries was validated by a suppressed estrus cycle.

3.4. *In vivo* measurements

3.4.1. Surgical procedures

Before the *in vivo* cerebrocortical or carotid artery blood flow measurements, a surgical preparation was performed under a

stereomicroscope. After body weight measurement, the left femoral artery was cannulated under isoflurane (2%) anesthesia to measure arterial blood pressure changes during the *in vivo* experiments. Then, ketamine-xylazine was injected intraperitoneally as an anesthetic, and a cannula was inserted into the trachea. The last step of the surgery depended on which *in vivo* experiment was performed subsequently: for the cerebrocortical blood flow measurement, a loose knot was placed around the left common carotid artery for later occlusion, whereas for the carotid artery blood flow measurement, flow probes were placed around both common carotid arteries and both external carotid arteries were ligated. Ketamine-xylazine was re-administered when necessary, and the body temperature was maintained at 37-38 °C.

3.4.2. Measurement of cerebrocortical blood flow using laser-speckle imaging

The *in vivo* cerebrocortical blood flow measurements were performed five weeks after OVX or after the testosterone treatment. 10 VDR^{Δ/Δ} and 10 WT intact mice were assigned to the control groups. CoBF changes induced by CAO were measured using laser-speckle imaging. After the surgery, the mouse was placed in a stereotaxic head holder, and a midline scalp incision was made to expose the skull, allowing the laser light to reach the cerebral cortex. Mean arterial blood pressure (MABP) was recorded using the femoral artery cannula. O₂ saturation, heart rate, and respiratory rate were monitored using a pulse oximeter placed on the right hindlimb. Atipamezole was injected to reverse the α -2-agonist effects of xylazine, and after the blood pressure stabilized, baseline CoBF and MABP were recorded for one minute. Then, the loose knot around the left carotid artery was tightened to induce the occlusion, and CoBF changes were recorded for five minutes. CoBF changes were measured in three cerebrocortical regions in both hemispheres (with the hemisphere on the side of the occlusion referred to as ipsilateral, while the other

hemisphere as contralateral): frontal, parietal, and temporal cortices. CoBF changes were expressed as a percentage of the baseline reference value (100 %), calculated as the average of baseline CoBF during the one-minute recording before CAO. Two phases of the adaptation were examined separately: 0-30 s after CAO was considered the acute phase, and 31-300 s was the subacute phase. To assess the CoBF reductions quantitatively, the area over the curve (AOC) was calculated for each animal for both phases (i.e., acute, subacute) and all regions. Arterial blood gas tensions ($p\text{CO}_2$, $p\text{O}_2$), acid-base parameters (pH, bicarbonate concentration), hematocrit, O_2 saturation, and plasma ion concentrations (Ca^{2+} , Na^+ , K^+ , Cl^-) were determined at the end of the measurements by radiometric analysis. Arterial blood samples were also collected for later serum testosterone concentration measurements. Heart weight, brain weight, and tibial length were measured after the experiments.

3.4.3. Measurement of carotid artery blood flow using transit-time ultrasonic flowmeter

Carotid artery blood flow measurements were performed in 8 $\text{VDR}^{\Delta/\Delta}$ and 6 WT intact female and 6 $\text{VDR}^{\Delta/\Delta}$ ♂ and 6 WT♂ male mice. Ultrasonic transit-time perivascular flow probes 0.5 PSB and TS420 flowmeter were used to measure carotid artery blood flow. Atipamezole was administered, and after stabilization, baseline blood flow and MABP were recorded for one minute. Then, a vessel clip was placed distally to the flow probe to occlude the left common carotid artery, and the contralateral carotid artery blood flow and MABP were measured for five minutes. Vascular conductance was calculated as the ratio of blood flow (mL/min) and MABP (mmHg). O_2 saturation, heart rate, and respiratory rate were monitored using a pulse oximeter.

3.5. Morphological analysis of leptomeningeal collaterals

The cerebrocortical vasculature was visualized in 5 $\text{VDR}^{\Delta/\Delta}$ and 6 WT intact female mice under isoflurane anesthesia (2%) by transcatheter perfusion with 10 mL of heparinized saline solution (10

IU/mL) followed by 2 mL of a mixture of black ink, endorsing ink and distilled water in the ratio of 6:1:6. Then, the brains were removed after decapitation, and fixed with formaldehyde solution (4%) for at least 24 hours. ImageJ software was used to evaluate the morphology of leptomeningeal collaterals that connect the branches of the anterior cerebral artery (ACA) and the middle cerebral artery (MCA) in digital images captured by a digital camera attached to the microscope. The number of collaterals, tortuosity index (the ratio of vessel curve length and the linear distance between the two ends of the vessel), and the distance between the anastomotic line (a line connecting the half-distance points between the nearest branching points of the ACA and MCA) and the midline were determined in each hemisphere.

3.6. Statistical analysis

The normal distribution of datasets was confirmed by the Shapiro-Wilk test, and the data are presented as mean \pm SEM. If the distribution of data was not normal, data are presented as median and interquartile range. The statistical significance of results obtained from the *in vivo* experiments was determined using two-way ANOVA followed by Bonferroni's or Tukey's post hoc test (depending on the number of variables). ANOVA was carried out after data transformation when the distribution of data was not normal. The significance of weight gain was assessed by the Student's paired t-test or Wilcoxon test. In the morphological analysis, p-values were calculated by the Student's unpaired t-test. GraphPad Prism software was used for statistical analysis, and $p < 0.05$ was considered a statistically significant difference.

4. Results

4.1. Anatomical and physiological features

4.1.1. Anatomical traits of females

Body weight, heart weight, brain weight, and tibial length were not different between intact VDR $^{\Delta\Delta}$ and WT females; however, VDR $^{\Delta\Delta}$

mice had shorter tibia lengths than OVX-WT (** $p < 0.01$) and TT-WT (* $p < 0.05$) mice. TT-WT mice had significantly higher body weight than intact WT (* $p < 0.05$), intact VDR Δ/Δ (** $p < 0.01$), OVX-VDR Δ/Δ (* $p < 0.05$), and TT-VDR Δ/Δ mice (* $p < 0.05$; two-way ANOVA followed by Tukey's post hoc test, $n=10$ in all groups). Additionally, both ovariectomy (OVX-VDR Δ/Δ : **** $p < 0.0001$, OVX-WT: ** $p < 0.01$, paired t -test, $n=10-10$) and the five-week testosterone treatment (TT-VDR Δ/Δ : *** $p < 0.001$, TT-WT: * $p < 0.05$, Wilcoxon test $n=10-10$) caused a significant increase in body weight.

4.1.2. Validation of testosterone treatment and ovariectomy

Although testosterone concentrations were below the detection limit (0.05 ng/mL) in the intact control (VDR Δ/Δ , WT) and ovariectomized groups (OVX-VDR Δ/Δ , OVX-WT), testosterone concentrations were well above the detection limit in both testosterone-treated groups, indicating the success of the transdermal treatment to induce androgen excess. Testosterone concentrations measured in the TT-WT (1.51 ± 0.25 ng/mL) and TT-VDR Δ/Δ (1.06 ± 0.18 ng/mL) groups were not significantly different from each other ($n=8-8$, unpaired t -test). The ovariectomized groups showed acyclicity five weeks after the removal of the ovaries, which confirmed the success of the surgery.

4.1.3. Morphology of leptomenigeal collaterals in intact females

The number of MCA-to-ACA collaterals was significantly smaller in VDR Δ/Δ females compared to WT mice (Figure 1A, $n(WT)=6$, $n(VDR\Delta/\Delta)=5$, where n refers to the number of brains analyzed, Student's unpaired t -test, * $p < 0.05$). However, the tortuosity (Figure 1B) and localization of the collaterals (Figure 1C) were not different between the experimental groups.

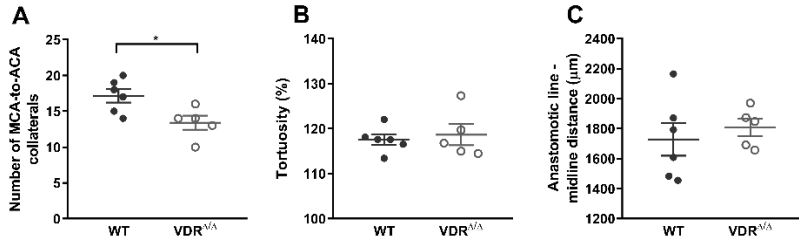


Figure 1. Morphological analysis of leptomeningeal collaterals in intact vitamin D receptor-mutant ($VDR^{\Delta/\Delta}$) and wild-type (WT) female mice.

4.2. *In vivo* measurements

4.2.1. Impact of vitamin D receptor deficiency and sex on the extracranial circulation

In male mice ($VDR^{\Delta/\Delta}\delta$, $WT\delta$), the blood flow similarly increased in the intact carotid artery after CAO (Figure 2A). Vascular conductance was also enhanced (Figure 2C), as no major changes were registered in MABP after CAO (Figure 2B). No significant differences were found between the male groups in these parameters (Figure 2, $n=6-6$, two-way ANOVA followed by Bonferroni's post hoc test).

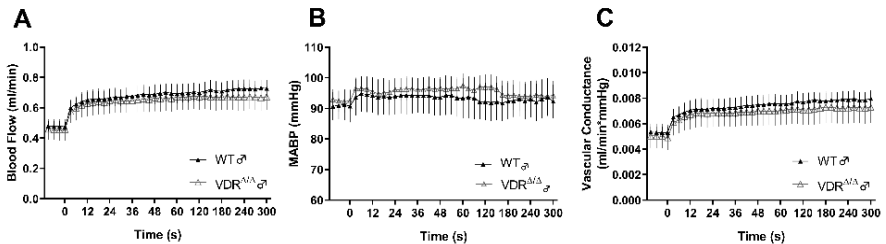


Figure 2. Changes of blood flow, mean arterial blood pressure (MABP), and vascular conductance in the intact contralateral carotid artery after unilateral carotid artery occlusion in male vitamin D receptor-mutant ($VDR^{\Delta/\Delta}\delta$) and wild-type ($WT\delta$) mice.

In female mice ($VDR^{\Delta/\Delta}$, WT), contralateral carotid artery blood flow similarly increased after CAO (Figure 3A). MABP was slightly affected by CAO (Figure 3B), and vascular conductance was increased (Figure 3C). No significant differences were found between the groups in these parameters (Figure 3, $n(WT)=6$, $n(VDR^{\Delta/\Delta})=8$, two-way ANOVA followed by Bonferroni's post hoc test).

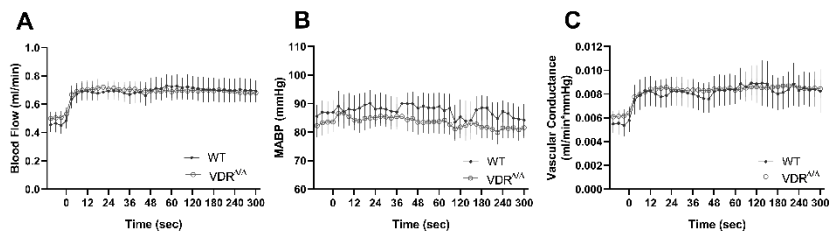


Figure 3. Changes of blood flow, mean arterial blood pressure (MABP), and vascular conductance in the intact contralateral carotid artery after unilateral carotid artery occlusion in female vitamin D receptor-mutant ($VDR^{\Delta/\Delta}$) and wild-type (WT) mice.

Heart rate, respiratory rate, and O_2 saturation were also monitored, and no significant differences were found in these parameters among the male and female groups.

4.2.2. Effects of vitamin D receptor deficiency and hormonal changes on the cerebrocortical blood flow changes after CAO in females

4.2.2.1. *In vivo* blood pressure measurements

No significant differences were found in MABP values among the experimental groups, and all MABP were in the physiological range and above the lower limit of cerebral autoregulation during the experiment. Therefore, we can rule out the possibility that MABP altered the cerebrovascular autoregulatory capacity in any of the experimental groups.

4.2.2.2. Analysis of blood gas, acid-base parameters, and plasma ion concentrations

Arterial blood gas (pCO₂, pO₂), acid-base parameters (pH, bicarbonate concentration), hematocrit level, plasma ion concentrations (Na⁺, K⁺, Ca²⁺, Cl⁻), and O₂ saturation analyzed in arterial blood samples were not different among the experimental groups. All parameters were within the physiological range; thus, we can rule out the possibility that they altered the cerebrovascular autoregulatory capacity in any of the experimental groups. Calcium ion concentrations were also similar in VDR-deficient and WT mice, which indicates that the rescue diet normalized calcium homeostasis in VDR-deficient mice.

4.2.2.3. Regional cerebrocortical blood flow changes after carotid artery occlusion

Figures 4A (ipsilateral hemisphere, which is on the side of the occlusion) and 4B (contralateral hemisphere) show the changes in CoBF after CAO in the frontal region. According to the calculated AOC values, no significant differences were discovered between the groups in the acute phase in the two hemispheres (Figure 4C, D). However, a considerable difference was observed in the subacute phase as the AOC values were higher in the TT-VDR^{Δ/Δ} group compared to intact females (VDR^{Δ/Δ}, WT) and OVX-WT mice, indicating that TT-VDR^{Δ/Δ} mice suffered a significantly prolonged reduction in blood flow in the ipsilateral hemisphere (Figure 4E, $n(WT)=10$, $n(VDR^{\Delta/\Delta})=8$, $n(OVX-WT)=9$, $n(OVX-VDR^{\Delta/\Delta})=10$, $n(TT-WT)=10$, $n(TT-VDR^{\Delta/\Delta})=9$, two-way ANOVA followed by Tukey's post hoc test, * $p<0.05$, ** $p<0.01$). No significant differences were found in the subacute phase of the contralateral side (Figure 4F).

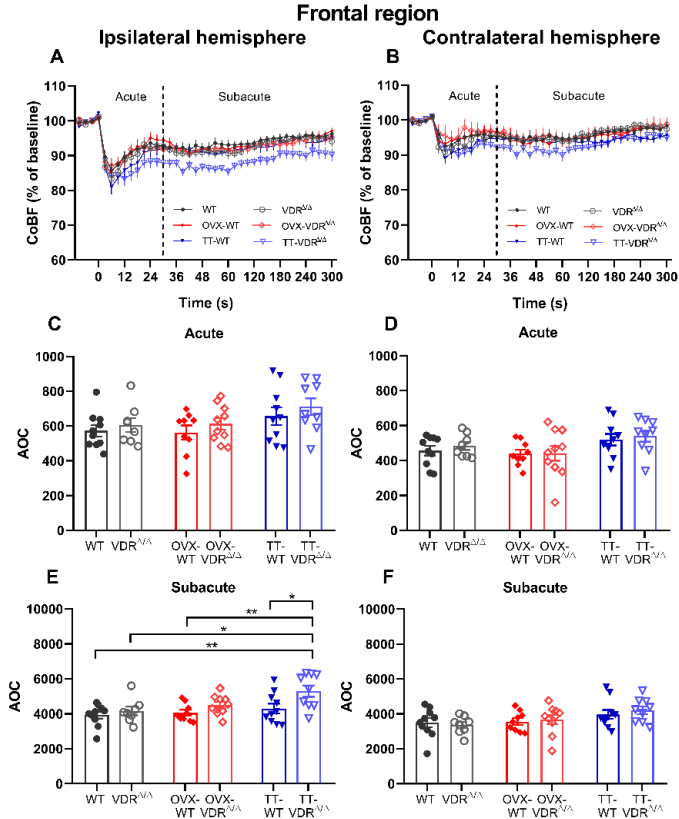


Figure 4. Cerebrocortical blood flow (CoBF) changes and area over the curve (AOC) values after unilateral carotid artery occlusion in the frontal cortex of intact, ovariectomized (OVX) and testosterone-treated (TT) vitamin D receptor-mutant ($VDR^{\Delta/\Delta}$) and wild-type (WT) female mice.

Figures 5A (ipsilateral hemisphere) and 5B (contralateral hemisphere) show the changes in CoBF after CAO in the parietal region. No differences were found between the groups in the acute phase (Figure 5C, D). However, in the subacute phase, TT- $VDR^{\Delta/\Delta}$ mice had higher AOC values on the ipsilateral hemisphere than WT and $VDR^{\Delta/\Delta}$ mice (Figure 5E, $n(WT)=10$, $n(VDR^{\Delta/\Delta})=8$, $n(OVX-WT)=9$, $n(OVX-VDR^{\Delta/\Delta})=10$, $n(TT-WT)=10$, $n(TT-VDR^{\Delta/\Delta})=9$, two-

way ANOVA followed by Tukey's post hoc test, $*p < 0.05$) indicating a delayed recovery. No significant differences were found in the subacute phase on the contralateral side (Figure 5F).

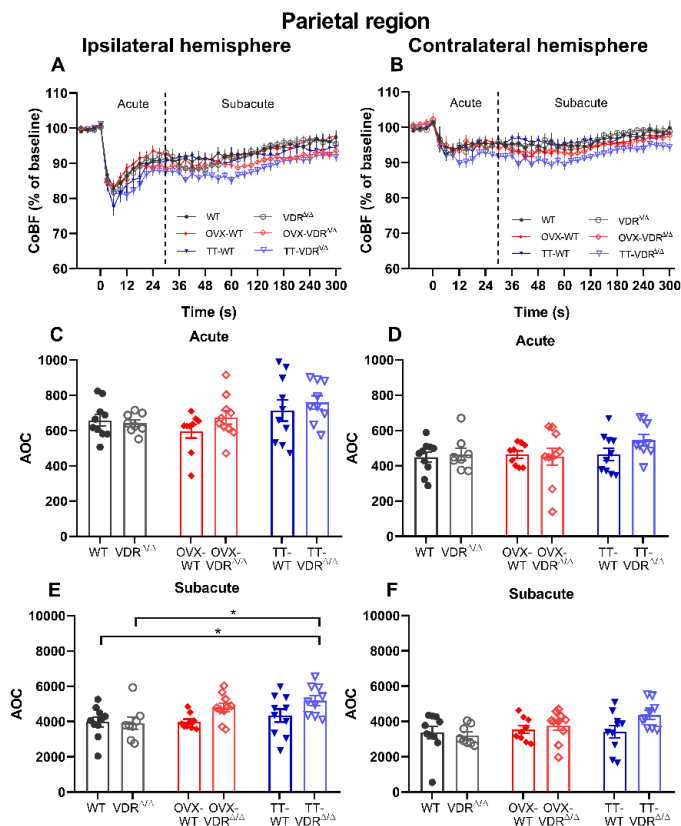


Figure 5. Cerebrocortical blood flow (CoBF) changes and area over the curve (AOC) values after unilateral carotid artery occlusion in the parietal cortex of ovariectomized (OVX) and testosterone-treated (TT) vitamin D receptor-mutant ($VDR^{\Delta/\Delta}$) and wild-type (WT) female mice.

Figures 6A (ipsilateral hemisphere) and 6B (contralateral hemisphere) show the changes in CoBF after CAO in the temporal region. No significant differences were observed between the groups in the acute phases (Figure 6C, D). However, higher AOC

values in the subacute phase in the ipsilateral hemisphere of the TT-VDR Δ/Δ group compared to the WT and OVX-WT groups indicate impaired adaptational capacity in TT-VDR Δ/Δ mice (Figure 6E, $n(WT)=10$, $n(VDR^{\Delta/\Delta})=8$, $n(OVX-WT)=9$, $n(OVX-VDR^{\Delta/\Delta})=10$, $n(TT-WT)=10$, $n(TT-VDR^{\Delta/\Delta})=9$, two-way ANOVA followed by Tukey's post hoc test, $*p<0.05$). No significant differences were found in the contralateral hemisphere in the subacute phase (Figure 6F).

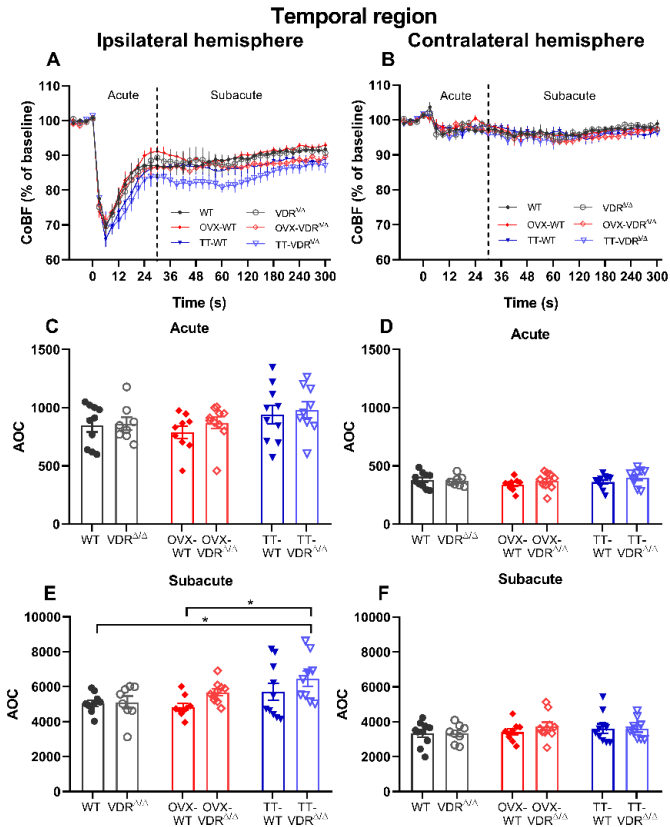


Figure 6. Cerebrocortical blood flow (CoBF) changes and area over the curve (AOC) values after carotid artery occlusion in the temporal cortex of intact, ovariectomized (OVX) and testosterone-treated (TT) vitamin D receptor-mutant (VDR Δ/Δ) and wild-type (WT) female mice.

5. Conclusions

We aimed to investigate the impact of disrupted vitamin D signaling and its interaction with altered sex hormone status on cerebrovascular adaptation to unilateral CAO. Our findings indicate that:

- In male mice, the compensatory increase in blood flow in the intact contralateral carotid artery after CAO was not compromised by VDR inactivity.
- Functional inactivation of VDR itself did not impair the cerebrovascular adaptation to CAO in intact females, to which may have contributed
 - the less severe morphological alterations of leptomeningeal collaterals and
 - the preserved reactivity of the intact contralateral carotid artery.
- Estrogen deficiency did not aggravate the effect of disrupted VDR signaling on the cerebrovascular adaptation to CAO.
- VDR-inactivity combined with hyperandrogenism impaired the acute blood flow compensation following CAO in female mice since the simultaneous presence of androgen excess and disrupted vitamin D signaling resulted in prolonged hypoperfusion in all regions of the ipsilateral cortex, implying a vasoregulatory dysfunction when vitamin D deficiency and hyperandrogenism coexist.

6. Bibliography of the candidate's publications

Publications related to the dissertation

Nagy D, Hricisák L, Walford GP, Lékai Á, Karácsony G, Várbíró S, et al. Disruption of Vitamin D Signaling Impairs Adaptation of Cerebrocortical Microcirculation to Carotid Artery Occlusion in Hyperandrogenic Female Mice. *Nutrients*. 2023;15(18):3869.

IF: 5.9

Pál É, Hricisák L, Lékai Á, **Nagy D**, Fülöp Á, Erben RG, et al. Ablation of Vitamin D Signaling Compromises Cerebrovascular Adaptation to Carotid Artery Occlusion in Mice. *Cells*. 2020;9(6).

IF: 6.6

Cumulative impact factor of the candidate's publications: **12.5**